PHILOSOPHICAL TRANSACTIONS A

Phil. Trans. R. Soc. A.
doi:10.1098/not yet assigned

Anisotropic magnetic hydrogels. Design, structure and mechanical properties

Cristina Gila-Vilchez[ab§], Mari C. Mañas-Torres [abc§], Rafael Contreras-Montoya[bc], Miguel Alaminos[bd], Juan D. G. Duran[ab], Luis Álvarez de Cienfuegos[bc], Modesto T. Lopez-Lopez[ab*†]

[a]*Department of Applied Physics, University of Granada, Avenida de la Fuente Nueva, 18071, Granada, Spain*
[b] *Instituto de Investigación Biosanitaria ibs.GRANADA, Granada, Spain*
[c] *Department of Organic Chemistry,University of Granada, Avenida de la Fuente Nueva, 18071, Granda, Spain*
[d] *Department of Histology (Tissue Engineering Group), University of Granada, Avenida de la investigación, 18016 Granada, Spain*

[§]*Both authors contributed equally to this study*

ORCID ID: CG-V, 0000-0002-8087-3770; MCM-T, 0000-0003-4673-5224; RC-M, 0000-0002-0766-004X; MA, 0000-0003-4876-2672; JDGD, 0000-0002-5586-1276; LAC, 0000-0001-8910-4241; MTL-L, 0000-0002-9068-7795

Keywords: magnetic hydrogels; polymers; magnetic particles; rheology; microstructure.

Summary

Anisotropy is an intrinsic feature of most of the human tissues (e.g. muscle, skin or cartilage). Because of this, there has been an intense effort in the search of methods for the induction of permanent anisotropy in hydrogels intended for biomedical applications. The dispersion of magnetic particles or beads in the hydrogel precursor solution prior to cross-linking, in combination with applied magnetic fields, which gives rise to columnar structures, is one of the most recently proposed approaches for this goal. We have gone even further and in this paper we show that it is possible to use magnetic particles as actuators for the alignment of the polymer chains in order to obtain anisotropic hydrogels. Furthermore, we characterize the microstructural arrangement and mechanical properties of the resulting hydrogels.

Introduction

Hydrogels are soft materials that can be defined as three dimensional, hydrophilic networks of flexible chains swollen by water or biological fluids. From a macroscopic physical point of view, hydrogels behave as viscoelastic solids, capable of enduring large mechanical deformations without fracture. This macroscopic feature is accompanied by a large porosity (even larger than 99 % in volume) at the microscopic level. As a consequence, provided the required biocompatibility, hydrogels recreate better than any other synthetic biomaterial the extracellular matrix of living tissues. Because of this, hydrogels are the focus of intense research in the materials science field, aiming to applications in biomedicine, especially as scaffolds for the regeneration of tissues by tissue engineering [1-4].

*Author for correspondence (modesto@ugr.es).
†Present address: Department of Applied Physics, University of Granada, Avenida de la Fuente Nueva, 18071, Granada, Spain

In spite of their resemblance to the extracellular matrix of living tissues, currently available synthetic hydrogels present important deficiencies that limit a full development of their potential applications in tissue engineering. Among them, the lack of appropriate mechanical properties and an adequate microstructural arrangement stand out [5]. From a general perspective, we could state that hydrogels with adequate (large) porosity to allow proliferation of cells and diffusion of nutrients and waste in the artificial growing tissues are mechanically too weak. On the contrary, when care is taken (for example by using strongly cross-linked, concentrated polymer networks) to prepare hydrogels that match the mechanical properties of target tissues the results are hydrogels with reduced porosity that hinders the proliferation of cells, and thus prevents for an appropriate generation of artificial tissues. Several approaches aimed at combining adequate mechanical properties and internal structures have been studied, including the use of inorganic nanomaterials in combination with polymers to strengthen the network without reducing the porosity [6-8].

Although, as discussed just above, the mechanical strength and degree of porosity of hydrogels intended to applications in tissue engineering are very important factors, not less relevant is their anisotropy, which is an aspect that is usually disregarded in most studies. In fact, most hydrogels are synthesized by homogeneous assembly of building blocks, resulting in isotropic networks, in contrast to most biological systems, such as muscle tissue [9, 10], skin tissue [11, 12], or cartilage tissue [13, 14], which present well-defined hierarchical, anisotropic structures. In these tissues anisotropy plays an essential role, making possible particular processes such as mass transfer, surface lubrication and force generation. As an example, muscle contraction results from the anisotropic disposition of actin-myosin within the sarcomere [9, 10]. Furthermore, it is also well-known that other processes, such as cell proliferation, migration and differentiation are also influenced by the anisotropy of the extracellular matrix of the host tissue [15-18].

Unfortunately, the preparation of anisotropic hydrogels by biocompatible processes is a difficult task, which requires the application of directional stimuli to the hydrogels, either during the building steps or after the finalization of the cross-linking process [19]. Examples include the application of mechanical strength [20, 21], magnetic or electric forces [19, 22, 23], as well as ionic or temperature gradients [19]. The application of mechanical strength is the most common method for inducing anisotropy and it can be easily conducted by subjecting the hydrogel to compression or traction along a given direction. As any viscoelastic material, hydrogels deform in response to mechanical strength, resulting in the appearance of anisotropy. Under certain conditions the deformation is maintained after the cessation of the strength, resulting in permanent anisotropy. For example, in the work by Scionti and co-workers [21] we demonstrated that when fibrin-based hydrogels were subjected to plastic compression between filter nylon membranes, the hydrogels were partially dehydrated resulting in the permanent alignment of the polymer fibres in parallel layers. Similarly, Mredha and co-workers [20] recently demonstrated that dehydration polymer hydrogels under high tensile stress induced perfectly aligned hierarchical fibrous structures. These anisotropic structures were maintained after cessation of the stress due to the appearance of lateral H-bonds between polymer fibres during drying. Unfortunately, these processes result in a reduction of porosity of the hydrogels and the consequent hindering of cell proliferation, as demonstrated for example for fibrin-based hydrogels [24].

By contrast to the case of mechanical strength, directional stimuli by application of electric or magnetic force fields does not require physical contact with the hydrogels, which represents a clear advantage. In these cases (electric or magnetic force fields), the directional stimuli are usually mediated by embedded nanoparticles, able to be oriented in an anisotropic way by the applied fields. A drawback of electric fields is that they may cause undesired electrochemical decomposition of the polymers. On the contrary, magnetic field can be safely used in the presence of polymers and even living cells [25]. To achieve manipulation of gels by magnetic forces, embedded nanoparticles must be of magnetisable material and their concentration must be high enough. As a consequence, the resulting gel presents a magnetisable character as a bulk. We refer to these systems as magnetic gels (hydrogels when they are water-based) or ferrogels, and from a microscopic point of view they are just suspensions of magnetic nanoparticles in a network of flexible chains swollen by a fluid [26-28]. Obviously, ferrogels possess the unique feature among soft matter of being responsive to magnetic fields, which allows not only non-contact manipulation, but also remote modification of their mechanical properties by magnetic fields [25].

In this paper, we focus on the use of magnetic nanoparticles for the preparation of biocompatible magnetic hydrogels. We will analyse three different cases of magnetic-field induced anisotropy. First, a magnetic supramolecular hydrogel, consisting of iron particles and Fmoc-diphenylalanine (Fmoc-FF) peptides that self-assemble by physical interactions in response to pH changes, in which anisotropy is obtained by the initial formation of nanoparticle columnar structures that are integrated within the hydrogel network. Second, a chemically cross-linked magnetic hydrogel, consisting of magnetite nanoparticles embedded in a network of fibrin polymers, in which anisotropy results as a consequence of the alignment during the cross-linking process of polymer fibres attached to magnetic nanoparticles. Finally, a magnetic alginate hydrogel, cross-linked by electrostatic bonding, in which anisotropy is induced by application of a magnetic field either before or after the cross-linking of the system, as a consequence of the tendency of magnetic materials to elongate in the direction of the magnetic field. In all three cases, anisotropy is obtained without dehydration of the sample, which represents a clear advantage with respect to methods based on the application of mechanical stress.

Anisotropic magnetic supramolecular hydrogels

Supramolecular hydrogels composed by short-peptides that assemble in response to external stimuli, such as changes in solvent or pH are excellent candidates for biomedical applications [29-31]. The inherent biocompatibility and biodegradability of peptides is one of the main advantages of hydrogels based on short-peptides. Furthermore, the great capacity to self-aggregate of peptides allows the formation of gels at very low gelator concentration to give soft materials composed, in some cases, by 99 % of water molecules. In addition, due to the non-covalent nature of peptide hydrogels (they assemble by various physical interactions such as hydrophobic, π-stacking, hydrogen bonding, etc.), they usually show shear-thinning behaviour [32]. Thanks to their shear-thinning behaviour peptide hydrogels can be administered *in vivo* by injection, avoiding surgical intervention. Also, they are excellent vehicles for the delivery of cells, since because their shear-thinning behaviour, when injected the shear rate is concentrated near the wall of the needle, protecting cells placed in the centre of the needle from damage cause by mechanical stress [32]. However, peptide hydrogels are usually too weak from the mechanical point of view and present a deficient microstructural arrangement, characterized by inhomogeneous pore size and poor reproducibility. Within this context, magnetic control seems an excellent alternative to improve the mechanical properties and microstructure of peptide hydrogels.

Design.

Peptide assembly is very sensitive to the experimental conditions and, as such, the simple introduction of nanoparticles may give rise to failure of hydrogel formation. Fortunately, we found that assembly of Fmoc-FF peptides took place in the presence of particles coated by polyethylene glycol (PEG). We used almost pure iron particles for this purpose of two different sizes. Iron nanoparticles (FeNPs) of diameter in the range 90 ± 30 nm, as well as iron microparticles (FeμPs) of 900 ± 300 μm. We coated both kinds of particles with a thin layer of PEG by following a water-in-oil emulsion method [33]. The PEG coating protects the iron core from corrosion and gives to the particles adequate biocompatibility, as demonstrated in a previous work [34]. Furthermore, PEG also showed affinity to Fmoc-FF peptide [35]. We made use of this affinity to integrate the particles within the hydrogel network. For this aim, we first suspended 100 mg of the PEG-coated particles in 1.5 mL of an aqueous basic solution of Fmoc-FF 0.5% (w/v), sonicated the resulting suspensions for 10 minutes and then centrifuged it for 5 min at 10000 rpm, discarding afterwards the supernatant, in order to recuperate the Fmoc-FF/PEG-coated particles. We will refer to these as FeNPs@PEG@Fmoc-FF and FeμPs@PEG@Fmoc-FF, respectively for the nanosized and microsized particles.

For the preparation of the magnetic hydrogels, we followed the protocol described in Ref. [35]. Briefly, we homogeneously dispersed by 5 min sonication, adequate amounts of either FeNPs@PEG@Fmoc-FF or FeμPs@PEG@Fmoc-FF in aqueous basic solutions of Fmoc-FF 0.5% (w/v), in order to obtain samples with

concentration of magnetic particles 0.6 vol.%. Then, we added 2 molar equivalents of glucono- δ-lactone (GdL) to the basic peptide solution, and homogenized again by 5 seconds of vortex mixer –GdL is weak acid that progressively decreased the pH of the suspension, provoking the gradual formation of peptide layers that eventually percolated, entrapping the water-media and thus building a hydrogel. Immediately afterwards, we placed the samples in the presence of a vertical magnetic field of 15 kA/m of strength. The application of the magnetic field induced the immediate chaining of the iron particles into columnar structures aligned in the direction of the applied field. After 1 hour the samples were already moderately cross-linked so that the magnetic field might be switched off without apparent collapse of the particle structures. The samples were left at rest for additional 23 hours in order to complete the gelation. For comparison we also prepared nonmagnetic hydrogels by following the same protocol without the addition of magnetic particles.

Kinetics of Gelation and Structure.

We monitored the gelation kinetics of the samples by subjecting them to oscillatory strain of 1 Hz of frequency and amplitude 0.001 during the 24 hours of gelling process. From these measurements we obtained the values of the viscoelastic moduli as a function of time. From the very beginning of the gelling process, the storage modulus (G') was higher than the loss modulus (G'') for both magnetic hydrogels and nonmagnetic hydrogels (data of G'' not shown here), which is an indication of the quick start of the gelation as soon as GDL was added.

The presence of magnetic particles was also evident from the very beginning of gelation, discerned by larger values of G' (much larger in the case of microparticles) in magnetic hydrogels than in nonmagnetic hydrogels (Figure 1a). This difference was without doubts due to the magnetic field-induced particle chaining. It should be noted, nevertheless, that particle migration in response to an applied magnetic field is a fast process that usually takes only a fraction of a second and, thus, differences in growth of G' with time after the first few minutes of gelation must be mainly due to differences in peptide-peptide and particle-peptide interactions. In fact, once aggregates of peptide-coated particles were built, it was expected that they acted as nuclei of condensation increasing cross-linking between peptide fibrils. Note that in a previous work [36] we showed for fibrin polymer hydrogels that properly functionalized particles acted as nuclei of condensation for the cross-linking of the polymers. The moment of switching off the applied magnetic field (3600 s) was clearly detected by the sharp drop in G' in the case of the magnetic hydrogel containing FeNPs@PEG@Fmoc-FF. In the case of the magnetic hydrogel containing FeμPs@PEG@Fmoc-FF, instead of a sharp drop followed by a smooth enhancement of G', a progressive decrement of G' with time for several hours was observed (see inserted plot in Figure 1a). Our hypothesis is that columnar structures built by microparticles were too heavy to be held by the peptide structure, which provoked a progressive, partial collapse. In fact, this agreed with direct observations that showed a not perfectly homogeneous hydrogel in this case. Note, nevertheless, that G' continued to be considerably higher for magnetic hydrogels even after switching off the field, which can be explained considering that the particle structures were engulfed by the peptides. At this point, it must be remembered that the particles were coated by peptides and thus, they might be integrated within the peptide network. It should finally be noticed the larger values achieved by the magnetic hydrogels at the stationary state.

The hypothesis of the formation of anisotropic magnetic field-induced particle structures in magnetic hydrogels, and their maintenance after the removal of the field, was confirmed by optical microscopy –see as an example Ref. [35], where particle chains of several microns of thickness were observed in an optical photograph for a magnetic hydrogel containing 0.01 vol.% of FeNPs@PEG@Fmoc-FF particles. By means of electron microscopy, we confirmed that FeNPs@PEG@Fmoc-FF particles were perfectly integrated within the peptide network [Figure 1b]. In fact, we could conclude that gelation of magnetic hydrogels results in anisotropic systems, characterized by the presence of thick columnar structures, composed by magnetic particles and peptide molecules, glued together by physical interactions between peptides themselves and the PEG coating of particles and peptides. These structures do not seem to affect the porosity of the hydrogels [35]. However, it should be noted that for FeμPs@PEG@Fmoc-FF particles, the interaction between particles in the presence of field was so strong that very thick particle structures, easily observable by naked eye, were

induced. These structures were not integrated so nicely as the structures of FeNPs@PEG@Fmoc-FF particles (see Figure 1c).

Mechanical properties.

We characterized the mechanical behaviour of both nonmagnetic and magnetic hydrogels in response to oscillatory shear strains (Figure 2). As observed, both nonmagnetic and magnetic hydrogels showed dependences of G′ and G′′ as functions of strain amplitude at a constant frequency of oscillation (Figure 2a), typical of gel-like systems. I.e., approximately constant values of G′, much higher than values of G′′, at low strain amplitude (a region known as linear viscoelastic region –LVR), followed by an increase of G′′ up to a maximum (maximum in dissipation of energy), which represents a yielding point, and a final drop of both magnitudes, G′ and G′′, as the value of strain amplitude further increased.
Similarly, the dependences of G′ and G′′ with frequency of strain oscillation at low amplitude (Figure 2b) equally presented typical values of cross-linked systems, characterized by viscoelastic moduli that increased smoothly with the value of the frequency. With respect to the relative magnitudes of G′ and G′′ for the different systems under study, as observed, the highest values are showed by magnetic hydrogels based on FeNPs@PEG@Fmoc-FF, whereas nonmagnetic hydrogels presented the lowest values. It should be noted at this point that no enhancement of the mechanical properties was obtained if magnetic hydrogels were prepared in the absence of applied field (isotropic magnetic hydrogels). The enhancement of the mechanical properties for these magnetic hydrogels can be explained by considering that the columnar structures are percolating. Applying the theoretical prediction for the mechanical properties of mixtures [37] we obtain:

$$G^{v}_{mix} = \Phi G^{v}_{c} + (1-\Phi) G^{v}_{m} \qquad (1)$$

where superscript v=′, ′′ correspond, respectively, for the storage and loss moduli, Φ is the volume fraction of columnar structures, and subscripts *mix*, *c*, *m* refer respectively to mixture, columnar structures and dispersion medium respectively. Concerning the fact that the enhancement of the viscoelastic moduli is stronger for nanoparticles than for microparticles, we may propose two complementary reasons. First, since the surface of the particles are coated by peptides and for a given amount of mass, nanoparticles have much larger (approximately ten times more) surface than microparticles, it is expected that integration of the particle structures is more effective for nanoparticles, which should result in a stronger enhancement. Secondly, since magnetic interaction is stronger for microparticles, the result for these particles was more the formation of columnar structures, mainly composed of particles, separated from the hydrogel medium, than the actuation of the particles as cross-linking agents between peptide fibres. Note also that the stronger the hydrogel (higher values of G′), the shorter the extension of the LVR. This result is somehow logical, since stronger systems are usually more rigid, and especially in the case of the present study, where strength of the magnetic hydrogels is related to the columnar structures built by the field and "glued" by the peptides. It is reasonable to consider these particles structures rather rigid.

Finally, let us mention that the anisotropy of the magnetic hydrogels was not limited to the appearance of a privileged direction, determined by the direction of the applied field, at the microscopic level, but also to the mechanical properties. In a previous work [35], we demonstrated for a magnetic hydrogel containing 0.3 vol.% of FeNPs@PEG@Fmoc-FF particles that shearing in a direction parallel to the columnar structures provided storage moduli about 5 times smaller than those obtained by shearing (like in the present work) in the perpendicular direction to the columnar structures.

Anisotropic fibrin-based magnetic hydrogels

Fibrin is a natural protein involved in the clotting of blood. Fibrin hydrogels are usually prepared by polymerization of fibrinogen obtained by blood plasma, resulting in polymer networks covalently cross-linked [38]. Due to their natural origin, fibrin-based hydrogels are intrinsically biocompatible and have been broadly used as scaffolds for the preparation of artificial tissues, including cornea, skin, oral mucosa, and peripheral nerve [39-43]. A main disadvantage of fibrin-based hydrogels is their mechanical weaknesses. To

overcome this problem and strengthen fibrin-based hydrogels, fibrin has been combined with other substances, either natural such as agarose [43, 44], or synthetic such as magnetic particles [36, 45, 46]. Additionally, fibrin-based hydrogels have been subjected to mechanical compression in order to reduce water content and thus enhance their mechanical properties.

Design.

Fibrin hydrogels were prepared by addition of Ca^{2+} ions to blood plasma, following the protocol first reported by Alaminos and coworkers [38]. Briefly, fibrin fibres are formed by polymerization of fibrinogen molecules, a process that takes place in three steps [36]. (i) Formation of fibrin monomers by thrombin cleavage of fibrinopeptides [47]. (ii) Formation of a non-covalent fibrin polymer network by electrostatic and hydrogen bonding between fibrin monomers. (iii) Covalent cross-linking of the fibrin polymer network, catalysed by the action of transglutaminase enzyme [47]. It should be noted that fibrinogen molecules are soluble before step (i) and contain some positively charged domains [47]. Therefore, they can interact electrostatically with negatively charged particles. In fact, we previously demonstrated that when magnetite nanoparticles with OH^- functionalization (MagP-OH nanoparticles from now on) were dispersed in the blood plasma prior to polymerization, these particles were homogeneously integrated within the resulting fibrin hydrogel, forming clusters at the knots of the polymer network [36]. These clusters very likely acted as condensation sites for the subsequent polymerization of the fibrin fibres, following steps (i) to (iii) described above.

For the preparation of the anisotropic magnetic fibrin hydrogels we used as a magnetic phase MagP-OH nanoparticles. These particles consisted of a spherical core of magnetite (90 vol.%) coated by a layer of polymer with OH^- functionalization. In total the particles have a mean hydrodynamic diameter of 110 nm, as measured by a Zetasizer instrument. We added adequate amounts of suspensions of these particles in phosphate buffered saline (PBS) buffer to liquid human plasma and homogenised the suspensions by mechanical shaking. Then, we added tranexamic acid (which is an antifibrinolytic drug) and a solution of $CaCl_2$, which initiated the polymerization process, as mentioned above –see more details in ref. [36]. Immediately afterwards, we poured the mixtures in culture dishes and placed them under the action of a vertical magnetic field of 48 kA/m of strength. The magnetic field was maintained during the first 5 minutes of polymerization. Finally, the samples were left to complete cross-linking for 24 hours under culture conditions (37 ◦C with 5% CO_2). In order to avoid dehydration, we added PBS to the samples 2 hours after the beginning of polymerization. For comparison, we prepared also isotropic magnetic hydrogels following the same protocol, but without the application of a magnetic field.

Kinetics of Gelation and Structure.

We monitored G′ and G′′ as a function of time for oscillatory strain of fixed amplitude (0.001) and frequency (1 Hz). As observed in Figure 3a, in all cases G′′ was higher than G′ at the beginning of the gelling process, although eventually there was a crossover and G′ become larger than G′′, indicative of a sol-gel transition (Figure 3a). The shortest time for the crossover of G′-G′′ (about 15 seconds) was observed for the anisotropic magnetic hydrogels (magnetic samples gelled for the first 5 minutes under a magnetic field), which is consistent with the existence of magnetic-field induced migration in these samples. The time required for the transition in the isotropic magnetic hydrogels (magnetic samples gelled in the absence of applied magnetic field) was about one order of magnitude longer (approx. 120 seconds), which was nevertheless considerably shorter than the time for the crossover in nonmagnetic samples (approx. 300 seconds). From this, we can conclude that the presence of the particles accelerated the kinetics of gelation and that this was even quicker under the application of a magnetic field.

In order to connect the kinetics of gelation with the microstructure, we carried out microscopic observation of the hydrogels after complete gelation (Figure 3). As observed, there are clear differences between the microstructure observed in the three samples. In the case of the anisotropic magnetic hydrogels, there was as expected an anisotropic structure, consisting of approximately parallel thick strips aligned in the direction of the applied magnetic field. On the contrary, for isotropic magnetic hydrogels and for nonmagnetic hydrogels there were isotropic structures. Nevertheless, in the case of nonmagnetic hydrogels (Figure 3d), the

microstructure consisted of polymer fibres randomly distributed, whereas in the case of isotropic magnetic hydrogels (Figure 3c), there were knots that cross-linked (each of them) several (of the order of 10) polymer fibres. These knots very likely consisted of clusters of nanoparticles and polymer fibres, which originated as a consequence of the interaction between particles and fibrinogen molecules in the suspensions of particles in plasma, and that grew during the polymerization process, as mentioned above in paragraph design. Consequently, we may expect that when a magnetic field was applied at the beginning of the polymerization (anisotropic magnetic hydrogels), due to the magnetic attraction between initial particle/fibrinogen aggregates, some elongated structures were built, which were maintained during the complete polymerization process, giving rise to anisotropic structures, as observed in Figure 3b. It should be noted that no large clusters were observed in Figure 3b, very likely because orientation started at the very beginning of the polymerization process, preventing the initial aggregates from serving as condensation nuclei and thus from a large growth, as observed in the case of magnetic gels not subjected to a field (Figure 3c). In this case, the initial aggregates should rather have served to stretch the initial branches of fibrin polymer, which agrees with the observed privileged direction not only of the large parallel strips observed in Figure 3b, but also of the polymer fibres composing these strips.

Mechanical properties.

Magnetic fibrin hydrogels presented superior mechanical properties as compared with nonmagnetic hydrogels [36, 47, 48]. In the particular case of the rigidity modulus (initial slope of the shear stress vs. shear strain curves under stationary conditions), the enhancement reached approximately one order of magnitude for a concentration of magnetic nanoparticles as tiny as 0.4 vol.% (Figure 4). As observed, the enhancement of the rigidity modulus was even higher for anisotropic magnetic hydrogels than for isotropic magnetic hydrogels –note that for anisotropic hydrogels, the shear strain was applied perpendicular to the direction of the parallel strips observed in Figure 3b. It should be noticed that this enhancement is much larger than the one predicted by the theory of mechanics of composite systems. The enhancement in the absence of applied field must be connected with the role of the clusters of particles as knots for the crosslinking of the polymer network. In fact, the classical theory of the elasticity of polymer networks predicts an increase of the rigidity modulus of a gel with the number of threads linked to each knot [49]. As observed in Figure 3c, the presence of these clusters of particles resulted in an enhancement of the number of chains linking with a single cluster, which would justify the enhancement observed for isotropic magnetic hydrogels. Note that we presented a theoretical model based on this hypothesis that semiquatitatively predicted the experimental trends for the rigidity modulus as a function of particle concentration [36]. As for the even higher enhancement of the rigidity modulus for anisotropic magnetic hydrogels, its origin must be connected to the presence of the parallel strips observed in Figure 3b. In fact, in a previous work we also developed a theoretical model which demonstrated that magnetic hydrogels consisting of percolating cylinders of dense phase dispersed in a more diluted environment presented strong enhancement of the rigidity modulus, in agreement with results in Figure 4 [48].

Anisotropic magnetic alginate hydrogels

Alginic acid and its salts, which are mainly obtained from the extracellular matrix of brown algae, are biocompatible, non-toxic, abundant in source, cheap and readily available materials which have therefore found great popularity in several fields such as biotechnology, food industry and pharmaceutical industry [50]. In the case of alginate hydrogels, gelation occurs via electrostatic interactions between carboxyl groups of the polymeric chains and calcium ions [51]. This suggests that the properties of alginate hydrogels can be easily modified by the control of the alginate and calcium ion concentrations. In contrast with the previously cited hydrogels, alginate hydrogels are strong, versatile, easily handling and adaptable biomaterials. In spite of the weakness of the ion bonds that form their structure, all the previous advantages, along with the easy incorporation of a magnetic phase, makes alginate hydrogels ideal candidates for their use in this context.

Design.

We explored two different ranges of size concerning the magnetic phase (nano- and micro-sized magnetic particles) embedded into the alginate hydrogels. In the first case, we used FeNPs@PEG as magnetic phase, whereas in the second one silica-coated iron particles (FeCC) (BASF, Germany) of diameter 1.4 ± 0.6 μm and saturation magnetization M_S = 1587 ± 2 kA/m were used.

To prepare the alginate ferrogels with FeNPs@PEG, we dissolved sodium alginate (Sigma Aldrich, USA) in miliQ water at a concentration of 4 wt%. We took 2.6 mL of that solution and added 7.8 mg of calcium carbonate ($CaCO_3$) (Sigma Aldrich, USA) and the magnetic powder needed depending on the desired concentration. This mixture was stirred by a vortex mixer and sonicated during 20 minutes until it was totally homogeneous. Then, the gelation process was initiated by the addition of 27.8 mg of D-glucono-δ-lactone (GDL) (Sigma Aldrich, USA). The final mixture was placed in a Petri dish and was left at rest at room temperature for 15 minutes. After that, it was placed between two neodymium (NdFeB) magnets (Webcraft GmbH, Germany) of dimensions 30 x 30 x 15 mm. Depending on the position of the magnets (Figure 5), we obtained the so-called "perpendicular" or "parallel" anisotropy. This way, we obtained hydrogels with the embedded magnetic particles aligned in different directions depending on the position of the magnets. Note that magnetic particles will form chain-like structures in the direction of the external magnetic field. Finally, the same volume (2.6 mL) of a solution 0.5 M of calcium chloride ($CaCl_2$) (Sigma Aldrich, USA) was added after 10 minutes in order to strengthen the polymeric network.

On the other hand, in order to avoid particle sedimentation due to their higher size, alginate hydrogels with FeCC particles were prepared using the two-step protocol described in [52]. Thus, we firstly prepared an alginate hydrogel taking 2 mL of a 1% w/v solution of sodium alginate, adding 3 mg of $CaCO_3$ and 10.7 mg of GDL, and leaving the mixture at rest at room temperature for 90 minutes after properly homogenization. Then, the just formed soft hydrogel was broken by vortex mixing and the desired amount of FeCC powder was added. The alginate hydrogel with the magnetic phase was sonicated during 10 minutes and placed in a Petri dish, resting at room temperature for 15 minutes before placing it between the NdFeB magnets to create the anisotropy. Finally, the same volume of a solution 45 mM of $CaCl_2$ was added after 10 minutes.

Mechanical properties.

Mechanical characterization of nonmagnetic and magnetic hydrogels with both FeNPs@PEG and FeCC magnetic particles was carried out in response to oscillatory shear strains, as previously described for anisotropic magnetic supramolecular hydrogels. For these systems, we studied the values of G' corresponding to the LVR at a constant frequency of oscillation of 1 Hz.

First of all, as observed in Figure 6a for hydrogels with FeNPs@PEG, "perpendicular" anisotropic hydrogels presented the lowest values of G', even lower than those of nonmagnetic hydrogels; whereas "parallel" anisotropic hydrogels showed intermediate values higher than those of nonmagnetic hydrogels but lower than magnetic isotropic hydrogels. Although the values are very close and the uncertainties are pronounced, we applied two-tailed t-student tests and checked that, at the 0.05 significance level, the difference among the mean values is significantly different in all cases. Other experiments with different concentrations of sodium alginate and magnetic particles were carried out without better results. As observed in Figures 6b and 6c, the arrangement of the FeNPs@PEG particles, aligned in the direction of the applied magnetic field, provides the sought anisotropy that explains the differences found in the mechanical properties. Nevertheless, the interaction between the magnetic particles or between the magnetic particles and the alginate fibres is probably not strong enough to ensure a striking effect of the anisotropy induced by this method.

In order to contrast this hypothesis, the viscoelastic moduli of anisotropic alginate hydrogels with FeCC particles were monitored and compared with those obtained in our previous work [52]. We could observe once again the formation of chain-like structures in the direction of the magnetic field applied during the preparation of the hydrogels (see Figs. 7b and 7c). Thus, we confirmed that induced anisotropy arises from the

arrangement of the magnetic particles in the internal structure of the hydrogel. In this case, and in the absence of an applied magnetic field during the measure (Fig. 7a), we always obtained higher values of G' for magnetic hydrogels than for nonmagnetic ones. In addition, the values obtained for anisotropic hydrogels were very similar to those in isotropic ones. Therefore, we do not observe significant differences between having or not this induced anisotropy. Nevertheless, when an external magnetic field of 282 kA/m of intensity was applied during the measure process, a high increase of G' appeared for hydrogels with anisotropy in the perpendicular direction of the magnetic field, whereas no differences were observed between hydrogels with anisotropy parallel with the magnetic field and isotropic magnetic hydrogels.

This effect corroborates the hypothesis that not only the spatial anisotropy is important, but also a strong interaction is fundamental in anisotropic hydrogels to provide a noticeable enhancement of their mechanical properties. An essential difference between the peptide-based and the fibrin-based systems studied in the previous paragraphs, and the alginate-based system of the current paragraph, is the fact that in the former systems a polymerization process that results in the effective integration of the particles within the 3D network took place. On the contrary, in the case of alginate-based system the hydrogel was built by the electrostatic cross-linking of the alginate molecules, mediated by the Ca^{2+} ions, resulting in the particles embedded within the polymer network, without the existence of an effective linkage between them and the polymer chains. Other factors, such as the application of a magnetic field might drive the appearance of anisotropy, as shown in Figure 7a. Thus, we may conclude that different experimental factors, such as polymer nature, particle coating, or gelation process, are decisive to create a system with proper interactions and therefore, satisfactory anisotropy.

Conclusions

We have presented in this manuscript three different approaches for the fabrication of anisotropic magnetic hydrogels. In all three cases, anisotropy was achieved by noncontact magnetic forces acting on the magnetic particles used in the formulation of the hydrogels, without dehydration of the hydrogels.

In the first approach, very short peptides (Fmoc-FF) were adsorbed on magnetic particles and these Fmoc-FF-coated particles were included in the hydrogel precursor mixture. Then, sol-gel transition was initiated by pH change and a magnetic field was immediately applied. According to results, in this case particle migration by the action of magnetic field took place quickly, so that anisotropy basically consisted of chains of particles that were perfectly integrated within the final peptide hydrogel. We found that anisotropic magnetic peptide hydrogels presented superior mechanical properties, characterized by higher rheological moduli, than nonmagnetic peptide hydrogels, and that this superior behaviour was a direct consequence of the anisotropic structure, since no differences were obtained for isotropic magnetic hydrogels with respect to nonmagnetic ones.

In a different approach, fibrinogen monomers were electrostatically bounded to magnetic particles and then the beginning of the polymerization process was induced, followed by the almost immediate application of a magnetic field. In this case, the results indicated that long polymer fibres were built prior to the magnetic field alignment, which resulted in a microstructure consisting of elongated bands aligned with the magnetic field, constituted by particles and polymer fibres presenting a privileged orientation. From the macroscopic point of view, this anisotropic magnetic hydrogels demonstrated stronger mechanical properties than isotropic magnetic hydrogels and much stronger than nonmagnetic hydrogels.

Finally, we also investigated anisotropic magnetic hydrogels prepared by polymerization of a mixture of magnetic particles and alginate polymer. Since particles were coated either by polyethylene glycol (PEG) or silica, and the precursor alginate ions were negatively charged in water, only weak hydrogen bonds between alginate macromolecules and particles was expected. Consequently, when anisotropy was pursued by application of a magnetic field, in this case not completely satisfactory results were obtained, even though the

existence of aligned structures at the microscopic level was corroborated. However, differences in the bulk mechanical properties in the absence of an applied magnetic field during measurements were marginal. Only the application of a moderate magnetic field during rheological measurements (magnetorheological measurements) resulted in much stronger rheological values than nonmagnetic hydrogels and clear anisotropic mechanical properties.

To conclude, we could state that anisotropy can be easily achieved in magnetic hydrogels by means of applied magnetic fields. Nevertheless, optimization of the anisotropic behaviour requires attraction between the particles and the polymer or peptide fibres, and adjustment of the experimental factors related to magnetic field application, so that magnetic field-induced migration drags not only particles, but also long filaments attached to them. The results of our work may be extrapolated to other polymer or peptide systems of interest. Given the importance of anisotropy in many biological processes, we expect a fast growth of the field of anisotropic hydrogels, both from a fundamental point of view, as well as from the perspective of applications.

Acknowledgments
The authors acknowledge Dr. A.B. Bonhome-Espinosa (Department of Applied Physics, University of Granada) for helpful discussion.

Funding Statement
C.G.V. acknowledges financial support by Ministerio de Ciencia, Innovación y Universidades and University of Granada, Spain, for her FPU17/00491 grant. She also received support from the Ministerio de Economía, Industria y Competitividad, MINECO, and Agencia Estatal de Investigación, AEI, Spain, cofounded by Fondo Europeo de Desarrollo Regional, FEDER, European Union, Project FIS2017-85954-R.
M.C.M.T. received support from the Ministerio de Economía, Industria y Competitividad, MINECO, and Agencia Estatal de Investigación, AEI, Spain, cofounded by Fondo Europeo de Desarrollo Regional, FEDER, European Union, Project FIS2017-85954-R.
R.C.M. received support from the Ministerio de Economía, Industria y Competitividad, MINECO, and Agencia Estatal de Investigación, AEI, Spain, cofounded by Fondo Europeo de Desarrollo Regional, FEDER, European Union, Project FIS2017-85954-R. He also received financial support from Junta de Andalucía, Spain, Project P12-FQM-790.
M.A. received support by the Spanish Plan Nacional de Investigación Científica, Desarrollo e Innovación Tecnológica, Ministry of Economy and Competitiveness (Instituto de Salud Carlos III), Grant No. FIS PI17/00391, co-financed by Fondo Europeo de Desarrollo Regional (ERDF-FEDER, EU), UE and by the Regional Ministry of Health, Junta de Andalucía, Spain, Grant No. CS PI-0257-2017.
J.D.G.D. received support from the Ministerio de Economía, Industria y Competitividad, MINECO, and Agencia Estatal de Investigación, AEI, Spain, cofounded by Fondo Europeo de Desarrollo Regional, FEDER, European Union, Project FIS2017-85954-R.
L.A.C. received support from the Ministerio de Economía, Industria y Competitividad, MINECO, and Agencia Estatal de Investigación, AEI, Spain, cofounded by Fondo Europeo de Desarrollo Regional, FEDER, European Union, Project FIS2017-85954-R.
M.T.L.L. received support from the Ministerio de Economía, Industria y Competitividad, MINECO, and Agencia Estatal de Investigación, AEI, Spain, cofounded by Fondo Europeo de Desarrollo Regional, FEDER, European Union, Project FIS2017-85954-R.

Data Accessibility
This article has no additional data.

Competing Interests
We have no competing interests.

Authors' Contributions

C.G.V.: substantial contributions to acquisition of data; drafting the article; final approval of the version to be published.
M.C.M.T.: substantial contributions to acquisition of data; revising the article critically for important intellectual content; final approval of the version to be published.
R.C.M.: substantial contributions to acquisition of data and analysis and interpretation of data; revising the article critically for important intellectual content; final approval of the version to be published.
M.A.: substantial contributions to conception and design; revising the article critically for important intellectual content; final approval of the version to be published.
J.D.G.D.: substantial contributions to conception and design, and analysis and interpretation of data; revising the article critically for important intellectual content; final approval of the version to be published.
L.A.C.: substantial contributions to conception and design, and analysis and interpretation of data; revising the article critically for important intellectual content; final approval of the version to be published.
M.T.L.L.: substantial contributions to conception and design, analysis and interpretation of data; drafting the article; final approval of the version to be published.

References

1. Gahawar AK, Peppas NA, Khademhosseini A. 2014. Nanocomposite Hydrogels for Biomedical Applications. *Biotechnology and Bioengineering* **111,** 441-453. (10.1002/bit.25160)
2. Ismail YA, Martínez JG, Al Harrasi AS, Kim SJ, Otero TF. 2011. Sensing characteristics of a conducting polymer/hydrogel hybrid microfiber artificial muscle. *Sensors and Actuators B* **160**, 1180-1190. (10.1016/j.snb.2011.09.044)
3. Park KM, Lee SY, Joung YK, Na JS, Lee MC, Park KD. 2009. Thermosensitive chitosan–Pluronic hydrogel as an injectable cell delivery carrier for cartilage regeneration. Acta Biomaterialia **5**, 1956-1965. (10.1016/j.actbio.2009.01.040)
4. Tibbitt MW, Anseth KS. 2009. Hydrogels as Extracellular Matrix Mimics for 3D Cell Culture. *Biotechnology and Bioengineering* **103,** 655-663. (10.1002/bit.22361)
5. Van Vlierberghe S, Dubruel P, Schacht E. 2011. Biopolymer-Based Hydrogels As Scaffolds for Tissue Engineering Applications: A Review. *Biomacromolecules* **12**, 1387-1408. (10.1021/bm200083n)
6. Rezwan K, Chen QZ, Blaker JJ, Boccaccini AR. 2006. Biodegradable and bioactive porous polymer/inorganic composite scaffolds for bone tissue engineering. *Biomaterials* **27**, 3413-3431. (10.1016/j.biomaterials.2006.01.039)
7. Haraguchi K, Takehisa T. 2002. Nanocomposite Hydrogels: A Unique Organic–Inorganic Network Structure with Extraordinary Mechanical, Optical, and Swelling/De-swelling Properties. *Adv. Mater.* **14**, 1120-1124. (10.1002/1521-4095(20020816)14:16<1120::AID-ADMA1120>3.0.CO;2-9)
8. Hu Z, Chen G. 2014. Novel Nanocomposite Hydrogels Consisting of Layered Double Hydroxide with Ultrahigh Tensibility and Hierarchical Porous Structure at Low Inorganic Content. *Adv. Mater.* **26**, 5950-5956. (10.1002/adma.201400179)
9. Weber A, Murray JM. 1973. Molecular Control Mechanism in Muscle Contraction. *Physiol. Rev.* **53**, 612-673. (10.1152/physrev.1973.53.3.612)
10. Huxley AF. 1974. Muscular contraction. *J. Physiol*. **243**, 1-43. (10.1113/jphysiol.1974.sp010740)
11. Madison KC. 2003. Barrier Function of the Skin: "La Raison d'Être" of the Epidermis. *J. Invest. Dermatol.* **121**, 231-241. (10.1046/j.1523-1747.2003.12359.x)
12. Proksch E, Brandner JM, Jensen J. 2008. The skin: an indispensable barrier. *Exp. Dermatol.* **17**, 1063-1072. (10.1111/j.1600-0625.2008.00786.x)
13. Poole AR, Kojima T, Yasuda T, Mwale F, Kobayashi M, Laverty S. 2001. Composition and Structure of Articular Cartilage: A Template for Tissue Repair. *Clin. Orthop. Relat. Res.* **391**, S26- S33.
14. Fox AJS, Bedi A, Rodeo SA. 2009. The Basic Science of Articular Cartilage: Structure, Composition, and Function. *Sports Health* **1**, 461-468. (10.1177/1941738109350438)
15. Prang P, Müller R, Eljaouhari A, Heckmann K, Kunz W, Weber T, Faber C, Vroemen M, Bogdahn U, Weidner N. 2006. The promotion of oriented axonal regrowth in the injured spinal cord by alginate-based anisotropic capillary hydrogels. *Biomaterials* **27**, 3560-3569. (10.1016/j.biomaterials.2006.01.053)

16. Zhang S, Greenfield MA, Mata A, Palmer LC, Bitton R, Mantei JR, Aparicio C, Olvera de la Cruz M, Stupp SI. 2010. A self-assembly pathway to aligned monodomain gels. *Nat. Mater*. **9**, 594-601.
17. McClendon MT, Stupp SI. 2012. Tubular hydrogels of circumferentially aligned nanofibers to encapsulate and orient vascular cells. *Biomaterials* **33**, 5713-5722. (10.1016/j.biomaterials.2012.04.040)
18. Marelli B, Ghezzi CE, James-Bhasin M, Nazhat SN. 2015. Fabrication of injectable, cellular, anisotropic collagen tissue equivalents with modular fibrillar densities. *Biomaterials* **37**, 183-193. (10.1016/j.biomaterials.2014.10.019)
19. Sano K, Ishida Y, Aida T. 2018. Synthesis of Anisotropic Hydrogels and Their Applications. *Angew. Chem. Int. Ed.* **57**, 2532-2543. (10.1002/anie.201708196)
20. Mredha TI, Guo YZ, Nonoyama T, Nakajima T, Kurokawa T, Gong JP. 2018. A Facile Method to Fabricate Anisotropic Hydrogels with Perfectly Aligned Hierarchical Fibrous Structures. *Adv. Mater.* **30**, 1704937. (10.1002/adma.201704937)
21. Scionti G, Moral M, Toledano M, Osorio R, Durán JDG, Alaminos M, Campos A, López-López MT. 2014. Effect of the hydration on the biomechanical properties in a fibrin-agarose tissue-like model. *J Biomed Mater Res Part A* **102A**, 2573–2582. (10.1002/jbm.a.34929)
22. Lu Q, Bai S, Ding Z, Guo H, Shao Z, Zhu H, Kaplan DL. 2016. Hydrogel Assembly with Hierarchical Alignment by Balancing Electrostatic Forces. *Adv. Mater.* **3**, 1500687. (10.1002/admi.201500687)
23. Chen S, Hirota N, Okuda M, Takeguchi M, Kobayashi H, Hanagata N, Ikoma T. 2011. Microstructures and rheological properties of tilapia fish-scale collagen hydrogels with aligned fibrils fabricated under magnetic fields. *Acta Biomater.* **7**, 644-52. (10.1016/j.actbio.2010.09.014)
24. Carriel V, Scionti G, Campos F, Roda O, Castro B, Cornelissen M, Garzón I, Alaminos M. 2017. In vitro characterization of a nanostructured fibrin agarose bio-artificial nerve substitute. *J Tissue Eng Regen Med* **11**, 1412-1426. (10.1002/term.2039)
25. Lopez-Lopez MT, Scionti G, Oliveira AC, Duran JDG, Campos A, Alaminos M, Rodriguez IA. 2015. Generation and Characterization of Novel Magnetic Field-Responsive Biomaterials. *PLoS ONE* **10**, e0133878. (10.1371/journal.pone.0133878)
26. Messing R, Frickel N, Belkoura L, Strey R, Rahn H, Odenbach S, Schmidt AM. 2011. Cobalt ferrite nanoparticles as multifunctional cross-linkers in PAAm ferrohydrogels. *Macromolecules* **44**, 2990-2999. (10.1021/ma102708b)
27. Ilg P. 2013. Stimuli-responsive hydrogels cross-linked by magnetic nano-particles. *Soft Matter* **9**, 3465–3468. (10.1039/C3SM27809C)
28. Bonhome-Espinosa AB, Campos F, Rodriguez IA, Carriel V, Marins JA, Zubarev A, Duran JDG, Lopez-Lopez MT. 2017. Effect of particle concentration on the microstructural and macromechanical properties of biocompatible magnetic hydrogels. *Soft Matter* **13**, 2928–2941. (10.1039/c7sm00388a)
29. Wang H, Yang Z. 2012. Short-peptide-based molecular hydrogels: novel gelation strategies and applications for tissue engineering and drug delivery. *Nanoscale* **4**, 5259-5267. (10.1039/C2NR31149F)
30. Seow WY, Hauser CAE. 2014. Short to ultrashort peptide hydrogels for biomedical uses. *Materials Today* **17**, 381-388. (10.1016/j.mattod.2014.04.028)
31. Yan C, Pochan DJ. 2010. Rheological properties of peptide-based hydrogels for biomedical and other applications. *Chem. Soc. Rev.* **39**, 3528-3540. (10.1039/B919449P)
32. Guvendiren M, Lu HD, Burdick JA. 2012. Shear-thinning hydrogels for biomedical applications. *Soft Matter* **8**, 260-272. (10.1039/C1SM06513K)
33. Chatterjee J, Bettge M, Haik Y, Chen CJ. 2005. Synthesis and characterization of polymer encapsulated Cu–Ni magnetic nanoparticles for hyperthermia applications. *J. Magn. Magn. Mater.* **293**, 303-309. (10.1016/j.jmmm.2005.02.024)
34. Rodriguez-Arco L, Rodriguez IA, Carriel V, Bonhome-Espinosa AB, Campos F, Kuzhir P, Duran JDG, Lopez-Lopez MT. 2016. Biocompatible magnetic core–shell nanocomposites for engineered magnetic tissues. *Nanoscale* **8**, 8138-8150. (10.1039/C6NR00224B)
35. Contreras-Montoya R, Bonhome-Espinosa AB, Orte A, Miguel D, Delgado-López JM, Duran JDG, Cuerva JM, Lopez-Lopez MT, Álvarez L. 2018. Iron nanoparticles-based supramolecular hydrogels to originate anisotropic hybrid materials with enhanced mechanical strength. *Mater. Chem. Front.* **2**, 686-699. (10.1039/C7QM00573C)
36. Bonhome-Espinosa AB, Campos F, Rodriguez IA, Carriel V, Marins JA, Zubarev A, Duran JDG, Lopez-Lopez MT. 2017. Effect of particle concentration on the microstructural and macromechanical properties of biocompatible magnetic hydrogels. *Soft Matter* **13**, 2928-2941. (10.1039/C7SM00388A)
37. Christensen RM. *Mechanics of Composite Materials*. Krieger Publishing Company, Malabar, 1991.

38. Ahmed TAE, Dare EV, Hincke M. 2008. Fibrin: A Versatile Scaffold for Tissue Engineering Applications. *Tissue Engineering Part B: Reviews* **14**, 199-215. (10.1089/ten.teb.2007.0435)
39. Alaminos M, Del Carmen Sanchez-Quevedo M, Munoz-Avila JI, Serrano D, Medialdea S, Carreras I, Campos A. 2006. Construction of a complete rabbit cornea substitute using a fibrin-agarose scaffold. *Invest Ophthalmol Vis Sci* **47**, 3311–3317. (10.1167/iovs.05-1647)
40. Sanchez-Quevedo MC, Alaminos M, Capitan LM, Moreu G, Garzon I, Crespo PV, Campos A. 2007. Histological and histochemical evaluation of human oral mucosa constructs developed by tissue engineering. *Histol Histopathol* **22**, 631–640. (10.14670/HH-22.631)
41. Carriel V, Garzon I, Jimenez JM, Oliveira AC, Arias-Santiago S, Campos A, Sanchez-Quevedo MC, Alaminos M. 2012. Epithelial and stromal developmental patterns in a novel substitute of the human skin generated with fibrin-agarose biomaterials. *Cells Tissues Organs* **196**, 1–12. (10.1159/000330682)
42. Carriel V, Garrido-Gómez J, Hernández-Cortés P, Garzón I, García-García S, Sáez-Moreno JA, Del Carmen Sanchez-Quevedo M, Campos A, Alaminos M. 2013. Combination of fibrin-agarose hydrogels and adipose-derived mesenchymal stem cells for peripheral nerve regeneration. *J Neural Eng* **10**, 026022. (10.1088/1741-2560/10/2/026022)
43. Rodriguez IA, Lopez-Lopez MT, Oliveira AC, Sanchez-Quevedo MC, Campos A, Alaminos M, Duran JDG. 2012. Rheological characterization of human fibrin and fibrin-agarose oral mucosa substitutes generated by tissue engineering. *J Tissue Eng Regen Med* **6**, 636–644. (10.1002/term.466)
44. Park SH, Park SR, Chung SI, Pai KS, Min BH. 2005. Tissue-engineered cartilage using fibrin/hyaluronan composite gel and its in vivo implantation. *Artificial Organs* **29**, 838–845. (10.1111/j.1525-1594.2005.00137.x)
45. Zhao HG, Ma L, Gao CY, Shen JC. 2009. A composite scaffold of PLGA microspheres/fibrin gel for cartilage tissue engineering: fabrication, physical properties, and cell responsiveness. *J Biomed Mater Res Part B - Appl Biomater* **88B**, 240–249. (10.1002/jbm.b.31174)
46. Eyrich D, Wiese H, Mailer G, Skodacek D, Appel B, Sarhan H, Tessmar J, Staudenmaier R, Wenzel MM, Goepferich A, Blunk T. 2007. In vitro and in vivo cartilage engineering using a combination of chondrocyte-seeded long-term stable fibrin gels and polycaprolactone-based polyurethane scaffolds. *Tissue Eng* **13**, 2207–2218. (10.1089/ten.2006.0358)
47. Hudry-Clergeon G, Marguerie G, Pouit L, Suscillon M. 1975. Models proposed for the fibrinogen molecule and for the polymerization process. *Thromb. Res*. **6**, 533-541.
48. Zubarev A, Bonhome-Espinosa AB, Alaminos M, Duran JDG, Lopez-Lopez MT. 2018. Rheological properties of magnetic biogels. *Arch Appl Mech*, 1-13. (10.1007/s00419-018-1450-2)
49. Rubinstein M, Colby RH. *Polymer Physics*. Oxford University Press, Oxford, 2003
50. Kuo CK, Ma PX. 2001. Ionically crosslinked alginate hydrogels as scaffolds for tissue engineering: Part 1. Structure, gelation rate and mechanical properties. *Biomaterials* **22**, 511–521. (10.1016/s0142-9612(00)00201-5)
51. Khotimchenko YS, Kovalev VV, Savchenko OV, Ziganshina OA. 2001. Physical–Chemical Properties, Physiological Activity, and Usage of Alginates, the Polysaccharides of Brown Algae. *Russian Journal of Marine Biology* **27**, 53–64. (10.1023/a:1013851022276)
52. Gila-Vilchez C, Bonhome-Espinosa AB, Kuzhir P, Zubarev A, Duran JDG, Lopez-Lopez MT. 2018. Rheology of magnetic alginate hydrogels. *J. Rheol.* **62**, 1083-1096. (10.1122/1.5028137)

Figure captions

Figure 1. (a) Examples of gelation kinetics of nonmagnetic peptide hydrogel, magnetic peptide hydrogel based on FeNPs@PEG@Fmoc-FF particles and magnetic peptide hydrogel based on FeμPs@PEG@Fmoc-FF. Note that similar general features were obtained for other aliquots of the same samples. (b), (c) Environmental Scanning Electron Microscopy (ESEM) images of magnetic supramolecular peptide hydrogels. (b) Magnetic hydrogel based on FeNPs@PEG@Fmoc-FF nanoparticles. (c) Magnetic hydrogel based on FeμPs@PEG@Fmoc-FF microparticles.

Figure 2. Dynamic response of hydrogels. (a) Viscoelastic moduli as a function of shear strain amplitude for oscillatory strains of 1 Hz of frequency. (b) Viscoelastic moduli as a function of shear strain frequency for oscillatory strains of amplitude 10^{-3}. Squares: nonmagnetic peptide hydrogel; circles: magnetic peptide hydrogels containing FeμPs@PEG@Fmoc-FF particles; triangles: magnetic peptide hydrogels containing FeNPs@PEG@Fmoc-FF particles. Full symbols represent the storage modulus; open symbols the loss modulus.

Figure 3. (a) Examples of gelation kinetics of nonmagnetic fibrin hydrogel (squares), isotropic magnetic fibrin hydrogel (circles), and anisotropic magnetic fibrin hydrogel (triangles). Storage modulus, G': full symbols; Loss modulus, G'': open symbols. Concentration of magnetic particles in magnetic hydrogels was 0.4 vol.%. (b), (c), (d) Environmental Scanning Electron Microscopy (ESEM) images of fibrin hydrogels. (b) Anisotropic magnetic fibrin hydrogels. (c) Isotropic magnetic fibrin hydrogels. (d) Nonmagnetic fibrin hydrogel. Bar length: 5 μm. The direction of the applied magnetic field in (b) is indicated by the arrow. Concentration of magnetic particles in magnetic hydrogels was 0.2 vol.%

Figure 4. Rigidity modulus of magnetic fibrin hydrogels for increasing concentration of magnetic nanoparticles (MNP). Blacksquare symbol: Nonmagnetic hydrogel. Bullet symbols: magnetic hydrogels gelled in the absence of magnetic field. Triangle symbols: magnetic hydrogels gelled for the first 5 min under the application of a magnetic field of 48.6 kA/m. The modulus of the nonmagnetic hydrogel is 75 Pa. Reprinted by permission from Springer Nature from Ref. [48]

Figure 5. Scheme of the position of the magnets with respect to the hydrogels in order to obtain (a) "perpendicular" or (b) "parallel" anisotropy.

Figure 6. (a) Storage modulus as a function of shear strain amplitude of magnetic hydrogels with 0.3 vol.% of FeNPs@PEG magnetic particles and fixed frequency of 1 Hz. □: Non-magnetic hydrogel. ■: magnetic hydrogels gelled in the absence of magnetic field (isotropic magnetic hydrogels). ◧: magnetic hydrogels with "perpendicular" anisotropy. ◨: magnetic hydrogels with "parallel" anisotropy. (b), (c) X-ray microtomography images of a magnetic hydrogel with 0.3% vol. of FeNPs@PEG particles. (b) Line of observation parallel to the direction of anisotropy –note the irregular spots, likely associated to the existence of percolating chain-like structures. (c) Line of observation perpendicular to the direction of anisotropy –note the filament-like pattern.

Figure 7. (a) Storage modulus as a function of shear strain amplitude (constant frequency of 1 Hz) of magnetic hydrogels with 5 vol.% of FeCC magnetic particles. □: Non-magnetic hydrogel. ■: magnetic hydrogels gelled in the absence of magnetic field. ◧: magnetic hydrogels with "perpendicular" anisotropy. ◨: magnetic hydrogels with "aligned" anisotropy. Bullet symbols refers to data taken during the application of an external magnetic field of H=282 kA/m, while squares refers to measures without an external magnetic field applied. (b), (c) Optical microscopy images of a diluted magnetic hydrogel with FeCC particles. (b) Line of observation perpendicular to the direction of anisotropy –note the filament-like pattern. (c) Line of observation parallel to the direction of anisotropy –note the irregular spots, likely associated to the existence of percolating chain-like structures.

Figure 1

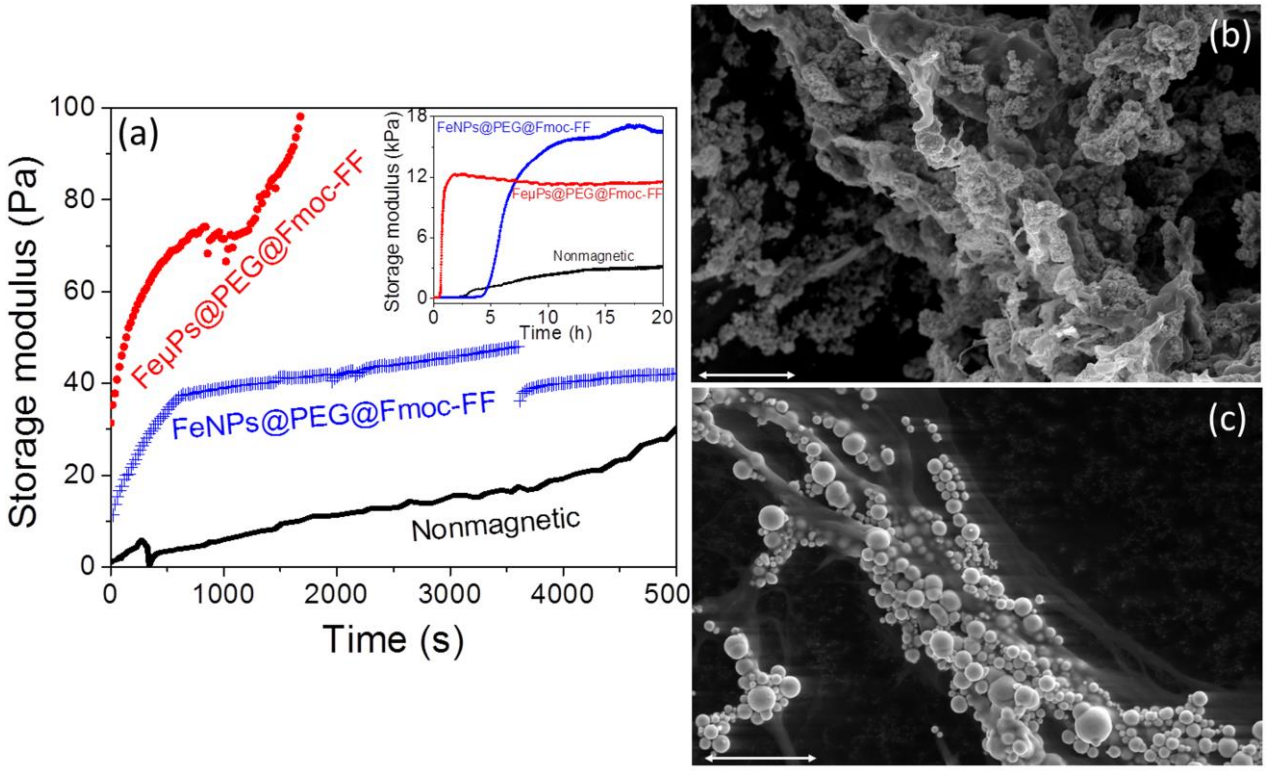
(a)
Storage modulus (Pa)
Time (s)
FeμPs@PEG@Fmoc-FF
FeNPs@PEG@Fmoc-FF
Nonmagnetic
Storage modulus (kPa)
Time (h)
(b)
(c)

Figure 2.

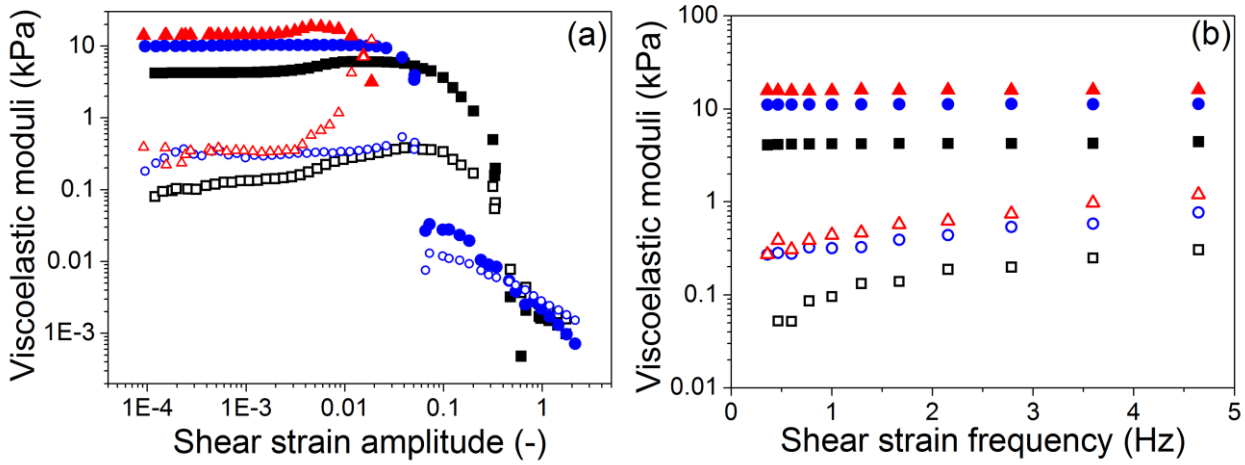
(a)
Viscoelastic moduli (kPa)
10
1
0.1
0.01
1E-3
1E-4
1E-3
0.01
0.1
1
Shear strain amplitude (-)
(b)
Viscoelastic moduli (kPa)
100
10
1
0.1
0.01
0
1
2
3
4
5
Shear strain frequency (Hz)

Figure 3.

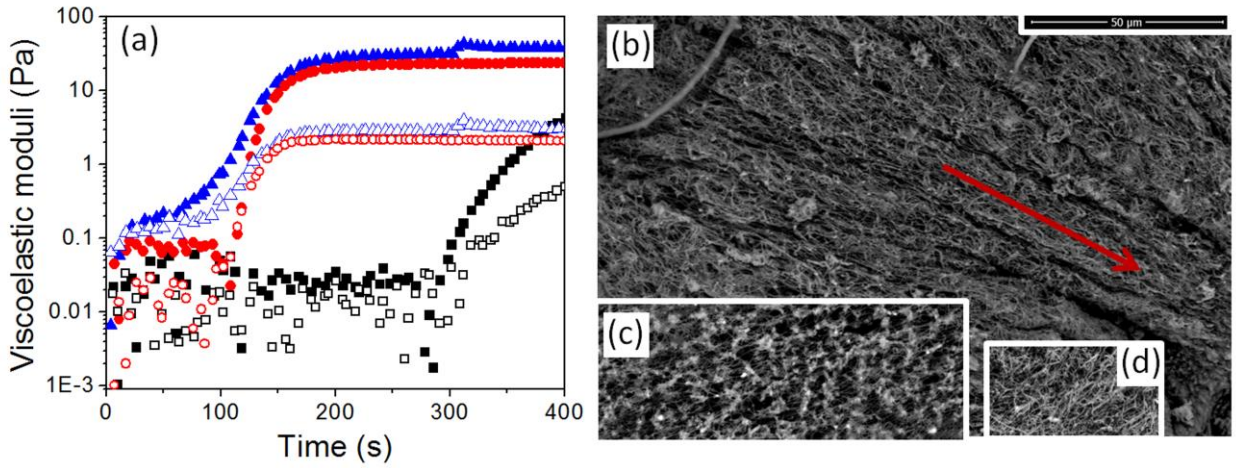
(a)
Viscoelastic moduli (Pa)
100
10
1
0.1
0.01
1E-3
0
100
200
300
400
Time (s)
(b)
50 µm
(c)
(d)

Figure 4.

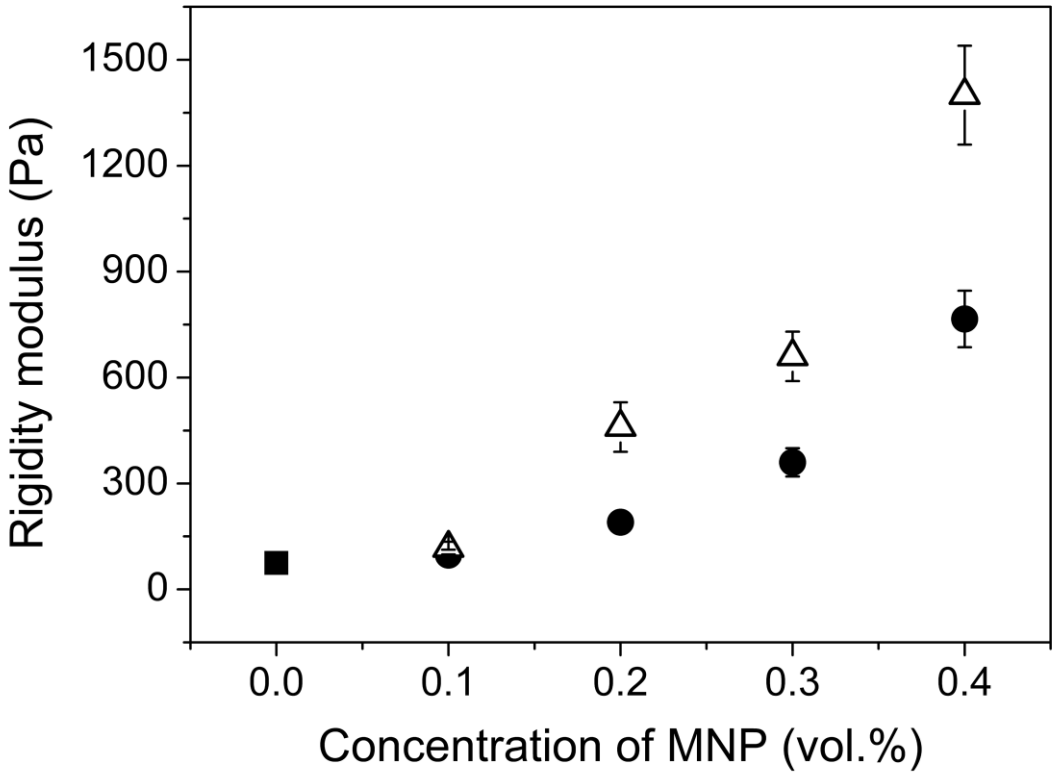
Rigidity modulus (Pa)
1500
1200
900
600
300
0
0.0
0.1
0.2
0.3
0.4
Concentration of MNP (vol.%)

Figure 5.

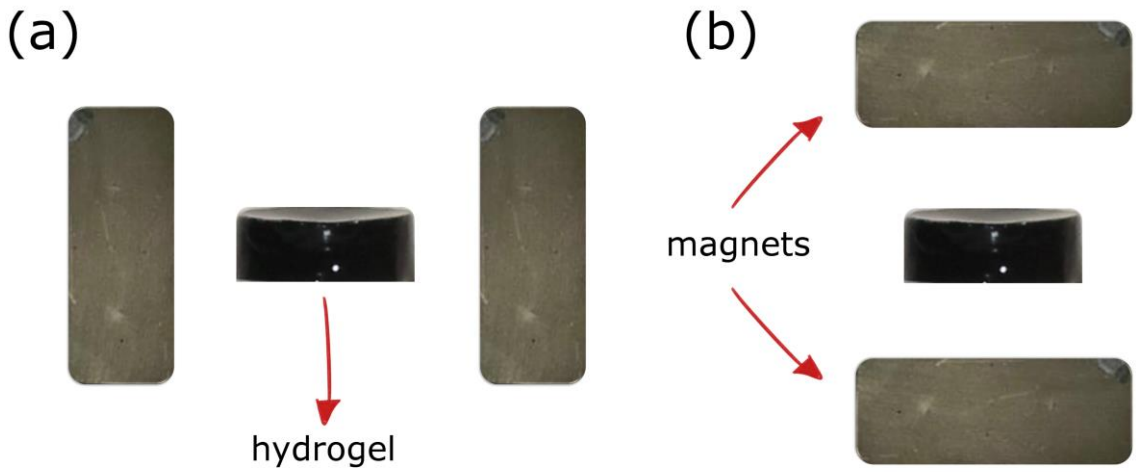

Figure 6.

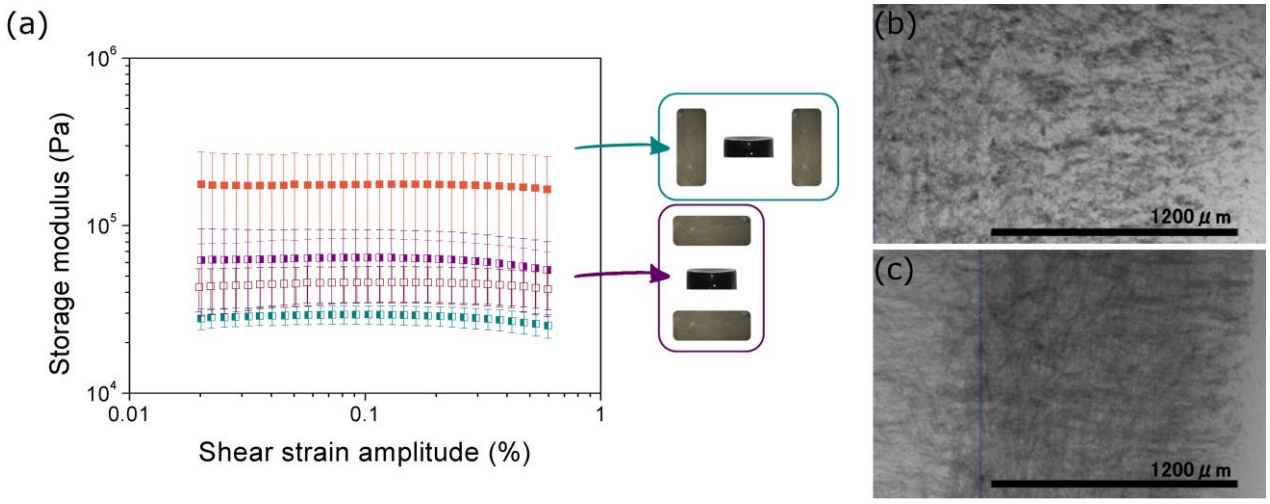
(a)
Storage modulus (Pa)
10^6
10^5
10^4
0.01
0.1
1
Shear strain amplitude (%)
(b)
1200 μm
(c)
1200 μm

Figure 7.

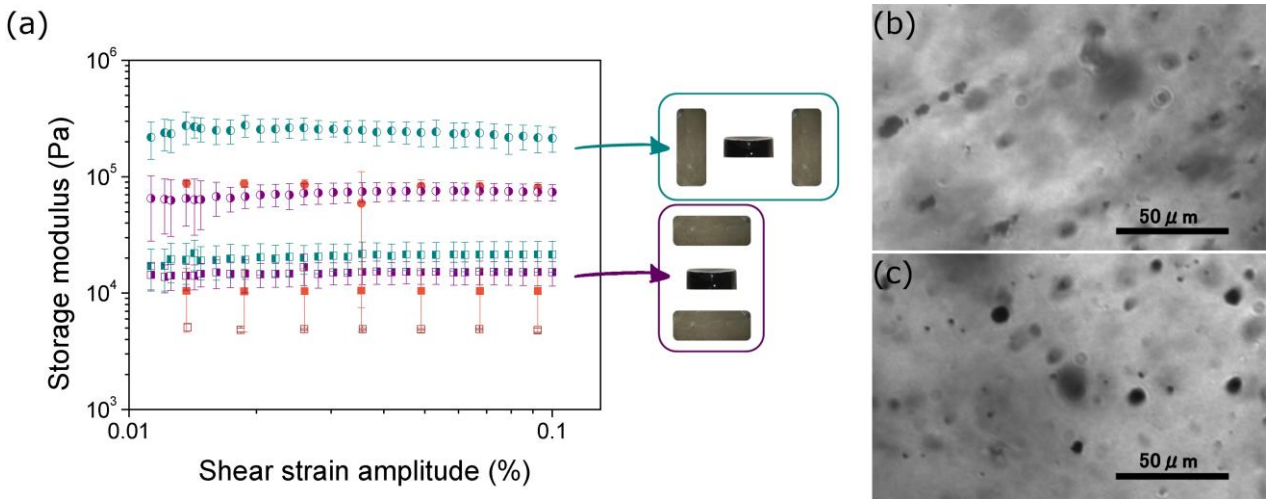
(a)
Storage modulus (Pa)
10^6
10^5
10^4
10^3
0.01
0.1
Shear strain amplitude (%)
(b)
50 μm
(c)
50 μm